Heterochromatin Controls γH2A Localization in Neurospora crassa

Citation	Sasaki, T., Lynch, K. L., Mueller, C. V., Friedman, S., Freitag, M., & Lewis, Z. A. (2014). Heterochromatin controls γH2A localization in Neurospora crassa. Eukaryotic Cell, 13(8), 990-1000. doi:10.1128/EC.00117-14
DOI	10.1128/EC.00117-14
Publisher	American Society for Microbiology
Version	Version of Record
Terms of Use	http://cdss.library.oregonstate.edu/sa-termsofuse

EC
Journals.ASM.org

Heterochromatin Controls γH2A Localization in *Neurospora crassa*

Takahiko Sasaki,[a] Kelsey L. Lynch,[a]* Caitlin V. Mueller,[a] Steven Friedman,[b] Michael Freitag,[b] Zachary A. Lewis[a]

Department of Microbiology, University of Georgia, Athens, Georgia, USA[a]; Department of Biochemistry and Biophysics, Center for Genome Research and Biocomputing, Oregon State University, Corvallis, Oregon, USA[b]

In response to genotoxic stress, ATR and ATM kinases phosphorylate H2A in fungi and H2AX in animals on a C-terminal serine. The resulting modified histone, called γH2A, recruits chromatin-binding proteins that stabilize stalled replication forks or promote DNA double-strand-break repair. To identify genomic loci that might be prone to replication fork stalling or DNA breakage in *Neurospora crassa*, we performed chromatin immunoprecipitation (ChIP) of γH2A followed by next-generation sequencing (ChIP-seq). γH2A-containing nucleosomes are enriched in *Neurospora* heterochromatin domains. These domains are comprised of A·T-rich repetitive DNA sequences associated with histone H3 methylated at lysine-9 (H3K9me), the H3K9me-binding protein heterochromatin protein 1 (HP1), and DNA cytosine methylation. H3K9 methylation, catalyzed by DIM-5, is required for normal γH2A localization. In contrast, γH2A is not required for H3K9 methylation or DNA methylation. Normal γH2A localization also depends on HP1 and a histone deacetylase, HDA-1, but is independent of the DNA methyltransferase DIM-2. γH2A is globally induced in *dim-5* mutants under normal growth conditions, suggesting that the DNA damage response is activated in these mutants in the absence of exogenous DNA damage. Together, these data suggest that heterochromatin formation is essential for normal DNA replication or repair.

Heterochromatin is comprised of transcriptionally repressed, repetitive DNA sequences that remain condensed throughout the cell cycle (1). The condensed structure of heterochromatin and the repetitive nature of heterochromatic DNA sequences pose challenges to genome integrity during DNA replication and DNA repair. Repeated DNAs are hot spots for various types of genome instabilities because they can adopt non-B-form DNA structures that stall replication forks and because they are common sites of illegitimate recombination (2–6). Such events can lead to mutations, gross chromosomal rearrangements, or copy number variations often associated with human diseases (7, 8). Despite their deleterious potential, repetitive DNA sequences make up a significant fraction of the genome in many eukaryotes, including many filamentous fungi (9–12). These sequences likely persist in genomes because they perform essential functions in certain contexts. For example, the centromeres of most eukaryotes are flanked by large, repeat-rich heterochromatin domains (13), and centromeres of the filamentous fungus *Neurospora crassa* are completely heterochromatic (14, 15). Thus, cells limit deleterious effects of repetitive DNA sequences while preserving essential functions of heterochromatin domains.

Heterochromatin in mammals and *N. crassa* is enriched with specific molecular markers, including histone H3 lysine-9 methylation (H3K9me), heterochromatin protein 1 (HP1), and cytosine DNA methylation. In *Neurospora*, heterochromatin formation is initiated at A·T-rich repetitive DNA sequences by the H3K9 methyltransferase DIM-5 (defective in methylation 5), which exists in a multiprotein complex called DCDC (DIM-5/7/9–CUL4/DDB1 complex) (16–19). According to proposed nomenclature conventions (20), DIM-5 is sometimes also referred to as KMT1 (lysine [K] methyltransferase 1), based on its structural and functional homologies with the mammalian Suv39H1 (KMT1A) and Suv39H2 (KMT1B) enzymes. By methylating H3K9, DIM-5^{KMT1} creates a binding site for multiple HP1-containing complexes, including the DIM-2 DNA methyltransferase complex (21), the HCHC histone deacetylase complex (HP1-chromodomain protein 2 [CDP-2]-histone deacetylase 1 [HDA1] complex) (22), and a complex containing a putative histone demethylase, DMM-1 (DNA methylation modulator 1) (23). The combined activities of these complexes are required for proper establishment and maintenance of heterochromatin domains in *Neurospora*. These domains include centromeres, subtelomeric regions, and hundreds of dispersed heterochromatin regions scattered throughout the genome (14, 15).

Proper heterochromatin formation appears to be important for normal genome stability in several organisms, but how specific heterochromatin components contribute to genome maintenance is not well understood (4). In the fission yeast *Schizosaccharomyces pombe*, replication fork stalling is observed in heterochromatin domains (24), and Clr4^{KMT1} mutants, which lack H3K9me, exhibit high rates of illegitimate recombination within the repetitive ribosomal DNA (rDNA) locus (25). Cytological studies in *Drosophila melanogaster* revealed that H3K9me-deficient mutants exhibit spontaneous double-strand breaks (DSBs) in heterochromatin domains (4, 26–28). H3K9me may promote genome stability through recruitment of HP1, as HP1 homologs in *Drosophila* and mammals contribute to the DNA damage response pathway through both H3K9me-dependent and -independent mechanisms (29–38). Recent work in *Neurospora* indicates that H3K9 methylation is important for genome maintenance in this fungus as well. DCDC-deficient mutants are hypersensitive to the DNA-damaging agent methyl methanesulfonate (MMS) (16), suggest-

Received 6 May 2014 Accepted 26 May 2014
Published ahead of print 30 May 2014
Address correspondence to Zachary A. Lewis, zlewis@uga.edu.
* Present address: Kelsey L. Lynch, Molecular and Cellular Biology Program, University of Washington, Seattle, Washington, USA.
Supplemental material for this article may be found at http://dx.doi.org/10.1128/EC.00117-14.

doi:10.1128/EC.00117-14

ing that H3K9 methylation may be important for DNA replication or DNA repair. To investigate this possibility further, we examined γH2A—a well-characterized marker of genotoxic stress—in wild-type strains and heterochromatin-deficient mutants.

In response to DNA replication stress or DNA DSBs, the mammalian H2A variant H2A.X is phosphorylated by ATM or ATR kinase on a serine near the C terminus (serine-139). The resulting modified histone, referred to as γH2AX, acts to stabilize stalled replication forks and facilitate double-strand-break repair (39). Fungi lack an H2A.X variant, but the core H2A protein contains an H2A.X-like sequence near the C terminus (SQEL). Similar to the situation in mammals, this C-terminal serine is phosphorylated by ATM and ATR kinases (Tel1 and Mec1 in *Saccharomyces cerevisiae*) to form γH2A in response to genotoxic stress (40). γH2A then recruits numerous chromatin-binding proteins to regulate genome stability (41).

Because γH2A accumulates around stalled replication forks and DSBs, this modified histone is often used as a marker of genome instability (42–45). In budding and fission yeasts, genome-wide analyses revealed that γH2A is enriched in heterochromatin domains during unperturbed vegetative growth (43, 45). Budding yeast (*S. cerevisiae*) lacks conserved features of heterochromatin, such as H3K9 methylation and HP1, but in *S. pombe*, γH2A was found to colocalize with H3K9me and HP1 (45). In the *S. pombe* $Clr4^{KMT1}$ mutant, γH2A enrichment was reduced in a heterochromatic region near the centromere and in a subtelomeric heterochromatin domain (45). In contrast, γH2A enrichment was unaffected in another heterochromatin domain, the silent mating-type locus. Thus, precisely how γH2A is directed to heterochromatin domains in either yeast species is not clear. In *Drosophila*, γH2A does not appear to be localized to heterochromatin domains in wild-type cells, but in H3K9-deficient mutants, high levels of γH2A are observed in heterochromatin domains, suggesting that heterochromatin-defective mutants suffer spontaneous DNA damage (26). In general, the functional and regulatory relationships between γH2A and heterochromatin are not well understood. We performed genomic, molecular, and cytological analyses of γH2A in *Neurospora*. We show that γH2A is a component of heterochromatin in *Neurospora* and that γH2A is significantly induced in a heterochromatin-defective mutant under normal growth conditions. These data suggest that ATM or ATR kinase is hyperactivated in the absence of normal heterochromatin. We propose that a repressive chromatin structure at repetitive, A·T-rich DNA sequences is important for normal genome stability in *Neurospora*.

MATERIALS AND METHODS

Strains and growth media. All *Neurospora* strains used in this study are listed in Table S1 in the supplemental material. Strains were grown at 32°C in Vogel's minimal medium (VMM) with 1.5% sucrose (46). Liquid cultures were shaken at 150 rpm. Crosses were performed on modified synthetic cross medium (46). For plating assays, *Neurospora* conidia were plated on VMM with 2.0% sorbose, 0.5% fructose, and 0.5% glucose. Where relevant, plates included 200 μg/ml hygromycin or 400 μg/ml Basta (47). LB medium supplemented with either ampicillin (50 μg/ml) or kanamycin (50 μg/ml) was used to grow *Escherichia coli* DH5α and XL1-Blue (48). Plasmids used for transformation were isolated using Qiagen miniprep kits.

Construction of H3K9 mutants. Primers used for site-directed mutagenesis are listed in Table S2 in the supplemental material. Primers were designed using previously described criteria (49). H3K9 mutations to glutamine or arginine were introduced by PCR, using plasmid pK9L as the template (50, 51). Plasmids containing *Neurospora* H3K9 mutations to glutamine or arginine were linearized with XbaI and introduced into *Neurospora* strain XStF9.1 by electroporation. This recipient strain contains the H3 coding sequence from *Fusarium graminearum* in place of the *Neurospora hH3* gene, as well as a deletion of *mus-51*. These features ensure that transformation leads to replacement of the entire *F. graminearum hH3* gene with the altered *Neurospora* H3 sequence. Homokaryotic H3 replacement strains were obtained by crossing primary transformants to the wild type. H3 replacement was confirmed by Southern blotting, followed by PCR and sequencing of the integrated DNA.

Molecular analyses. *Neurospora* transformation (52), DNA isolation (53), protein isolation, histone isolation, and Western blotting (54) were performed as previously described. Southern blotting was performed as described previously (55), except that probe synthesis, hybridization, and detection were carried out using a North2South chemiluminescence hybridization and detection kit (Thermo). Chemiluminescent blots were imaged using a ProteinSimple FluorChem E imager. Primers used to generate probe templates are listed in Table S2 in the supplemental material. Chromatin immunoprecipitation (ChIP) was performed using 5-hour-old germinating conidia. Fifty-milliliter cultures containing 5×10^6 conidia/ml were grown for 5 h, and conidia were harvested by centrifugation. Conidia were washed once in phosphate-buffered saline (PBS), and chemical cross-linking was performed by incubating conidia in PBS containing 1% formaldehyde at room temperature on a rotating platform for 30 min. The reaction was quenched with 125 mM glycine. Conidia were washed with PBS twice and resuspended in lysis buffer (50 mM HEPES, pH 7.5, 140 mM NaCl, 1 mM EDTA, 1% Triton X-100, 0.1% deoxycholate). For γH2A ChIP assays, the extraction buffer was supplemented with phosphatase inhibitor cocktail (Sigma). Chromatin was sheared by sonication, using an UltraSonic processor (duty cycle, 80; output, 3.5) (Heat System-Ultrasonics Inc.) to deliver 150 1-s pulses at 4°C. Lysates were centrifuged at 13,000 rpm for 5 min at 4°C. For γH2A-ChIP, 2 μl of anti-γH2A antibody (ab15083; Abcam) was used. For detection of H3K9 trimethylation (H3K9me3), 1 μl of antibody (Active Motif) was used. Protein A/G beads (20 μl) (sc-2003; Santa Cruz) were added to each sample. Following overnight incubation, beads were washed twice with 1 ml lysis buffer, once with lysis buffer containing 500 mM NaCl, once with 50 mM LiCl, and finally with TE (10 mM Tris-HCl, 1 mM EDTA). Bound chromatin was eluted in TES (50 mM Tris, pH 8.0, 10 mM EDTA, 1% SDS) at 65°C. Chromatin was de-cross-linked overnight at 65°C. The DNA was treated with RNase for 2 h at 50°C, treated with proteinase K for 2 h at 50°C, and extracted using phenol-chloroform. DNA pellets were washed with 70% ethanol and resuspended in TE buffer. Samples were then prepared for Illumina sequencing or subjected to analysis by quantitative real-time PCR.

qPCR and Illumina sequencing. Primers used for quantitative PCR (qPCR) are listed in Table S2 in the supplemental material. DNAs obtained from ChIP assays were diluted 1:50 in H_2O for input samples and 1:10 in H_2O for samples immunoprecipitated with H3K9me3, H3K4me2, or γH2A antibody. For PCR, iTaq Universal SYBR green Supermix (Bio-Rad) was mixed with specific primer pairs, and 1 μl of the diluted ChIP DNA was added. qPCR was performed using an iCycler IQ instrument (Bio-Rad). Statistical analyses were performed in Microsoft Excel. For Illumina sequencing, libraries were prepared using half of the total immunoprecipitated fraction following the instructions supplied with Illumina Tru-seq kits, except that genomic DNA adaptors were diluted 1:100 prior to ligation. Illumina sequencing was performed using an Illumina Hi-Seq 2000 genome analyzer at the University of Missouri DNA Core Laboratory.

Data analysis. Sequence reads were mapped to the latest *Neurospora* genome annotation (version 12), available from the *Neurospora* genome database (11), by using bowtie2 (56). Read numbers were counted for 25-bp bins by using igvtools, and the read density was visualized using the Integrated Genome Viewer (IGV), available from the Broad Institute

website (57, 58). We used IGV to normalize data to the total read number before plotting. To calculate normalized enrichment values, we created a custom feature annotation file containing genes, tRNAs, and DNA repeats. Repeated DNA sequences were identified by analyzing the *Neurospora* genome with RepeatScout (59). Repeat families were aligned to the *Neurospora* genome by using BLAT (60), and then coordinates were parsed using a custom perl script into a gene prediction format file that also contained coordinates for genes and tRNAs (downloaded from the Broad Institute genome database [11]). To calculate the normalized ChIP enrichment values (NLCS values) for each feature, we used EpiChIP software, which calculates enrichment values normalized for total read number and for length of the feature (61). Normalized H3K9me3, H3K4me3, and γH2A values for each feature were used to generate scatterplots and to calculate Pearson's correlation coefficients in Microsoft Excel. In addition, the NLCS values were used to plot the kernel density estimations for all features, genes, and repeats, using R (http://www.r-project.org). Where relevant, mapped reads were converted to bed format by use of bedtools software (62). Heterochromatin domains were classified as individual peaks by use of r-seg software (http://smithlabresearch.org/software/rseg/). The coordinates of H3K9me peaks are listed in Table S3 in the supplemental material.

Immunofluorescence. For cytological analysis of γH2A, we adapted a method previously described for *Aspergillus nidulans* (63). Conidia were inoculated into VMM containing 1.5% sucrose and incubated at 32°C for 12 h on coverslips or in an 8-well μ-Slide (Ibidi). Cells were fixed for 30 min in a solution containing 3.5% formaldehyde, 5% dimethyl sulfoxide (DMSO), 25 mM EGTA, and 5 mM $MgSO_4$. Fixed cells were washed with PBS three times, followed by a 90-min incubation in a 50% egg white solution containing 50 mM piperazine-*N*,*N*′-bis(2-ethanesulfonic acid) (PIPES), pH 6.7, 25 mM EGTA, 5 mM $MgSO_4$, 1 mM dithiothreitol (DTT), and 1 mg/ml of lyticase (purified from *Oerskovia xanthineolytica* [64]; generously provided by Vincent Starai, University of Georgia). Cells were washed again with PBS and incubated overnight at 4°C in a PBS solution containing the primary antibody (1:200 dilution of the Abcam anti-γH2A antibody described above). Cells were washed three times with PBSA (PBS supplemented with 0.1% bovine serum albumin [BSA]) and incubated for 50 min at room temperature in PBS containing a 1:200 dilution of the secondary antibody [Alexa Fluor 488–goat anti-rabbit IgG(H+L); Life Technologies]. Cells were washed with PBSA three times prior to imaging. Microscopy was performed using a DeltaVision II microscope equipped with a Delta Vision standard filter set, which includes fluorescein isothiocyanate (FITC) and tetramethyl rhodamine isocyanate (TRITC) filters for green and red fluorescence acquisition, respectively. Quantitative analysis of fluorescence intensities was performed using Softworx 1.3 software (Applied Precision).

Nucleotide sequence accession numbers. Sequence data from this study are available through the NCBI Short Read Archives (accession no. SRP042169).

RESULTS

γH2A is localized to heterochromatin domains in *Neurospora crassa*. γH2A is a functionally conserved modification of H2A that acts to stabilize replication forks and facilitate double-strand-break repair in fungi and animals (43–45, 65). To determine if γH2A is enriched at specific genomic locations in the filamentous fungus *Neurospora crassa*, we performed ChIP of γH2A followed by high-throughput sequencing (ChIP-seq). We used a previously characterized anti-γH2A antibody that was specific for both yeast and *Neurospora* γH2A proteins (H2A proteins phosphorylated on serine-129 and serine-131, respectively) (66, 67). We also performed ChIP-seq experiments to detect two well-characterized chromatin modifications, H3K4me2 and H3K9me3, which are molecular markers of euchromatin and heterochromatin, respectively. As expected, H3K4me2 was enriched in active genes, while H3K9me3 was localized to A·T-rich, gene-poor heterochromatin domains (Fig. 1A). γH2A enrichment was highly correlated with heterochromatin domains identified by enriched H3K9 trimethylation (Fig. 1A and B; see Fig. S1 in the supplemental material). To validate the ChIP-seq results, we performed qPCR to examine γH2A at representative euchromatin (*hH4* and *cfp*) and heterochromatin (8:A6 and 9:E1) domains. qPCR results were fully consistent with our ChIP-seq data, confirming that γH2A is a component of heterochromatin domains in *Neurospora* (Fig. 1C). To confirm that the γH2A antibody was specific, we performed ChIP experiments using a γH2A-deficient strain in which the single H2A gene was replaced with an H2A allele containing a serine-131-to-alanine substitution (66). Heterochromatic domains were not enriched in the $hH2A^{S131A}$ strain when qPCR analyses were performed for representative heterochromatic and euchromatic regions (Fig. 1C). Similarly, heterochromatin domains were not enriched when the entire γH2A immunoprecipitate fraction was assayed by ChIP-seq (Fig. 1A and B; see Fig. S1), demonstrating that the γH2A antibody was specific for phosphorylated H2A serine-131.

To validate that γH2A is localized with H3K9me3 at divergent repeated sequences throughout the genome, we used EpiChIP software (61) to calculate the NLCS values for all features in the genome. Features included genes, tRNAs, and repeated DNA sequences. We generated a scatterplot to compare the NLCS values for H3K9me3 and γH2A or to compare H3K4me2 and γH2A in genes and repeats. H3K9me3 and γH2A were similarly enriched in repeats, while exhibiting low levels of enrichment in genes (Fig. 1D) (Pearson's correlation coefficient = 0.80). In contrast, H3K4me2 was enriched in many of the genes and exhibited no correlation with γH2A (Fig. 1D) (Pearson's correlation coefficient = −0.16). We also calculated the kernel density estimations to examine the relative frequencies of enriched and unenriched features for H3K4me2, H3K9me3, and γH2A. Plotting the kernel densities revealed a bimodal distribution for all three modifications. In each case, one peak corresponds to features with background levels of enrichment, while the second peak represents features enriched with the modification. We also plotted the kernel densities for genes or repeats alone. For H3K4me2, genes were distributed in two peaks, corresponding to background and enriched features, while repeats were distributed in a single background peak (see Fig. S2A in the supplemental material). For both H3K9me3 and γH2A, genes were distributed in a single peak corresponding to background enrichment. In contrast, repeats were distributed in a single peak corresponding to enriched features (Fig. 2A and B). As expected, the kernel density estimation of γH2A enrichment in the $hH2A^{S131A}$ strain produced a single peak corresponding to uniform background enrichment for all features across the genome (Fig. 2C). However, the enrichment value observed for repeats was slightly lower than that for genes due to a subtle bias against A·T-rich sequences observed in Illumina sequencing experiments (68, 69). Together, these data demonstrate that γH2A localizes to repeat-rich heterochromatin domains across the *Neurospora* genome.

H3K9 methylation is required for normal γH2A localization. H3K9 methylation by $DIM\text{-}5^{KMT1}$ is an early step in heterochromatin formation (50, 70). We were interested to learn if γH2A localization depends on $DIM\text{-}5^{KMT1}$ or its enzymatic product, H3K9me3. We performed γH2A ChIP-seq experiments with a *dim-5* deletion strain and found that enrichment of γH2A was

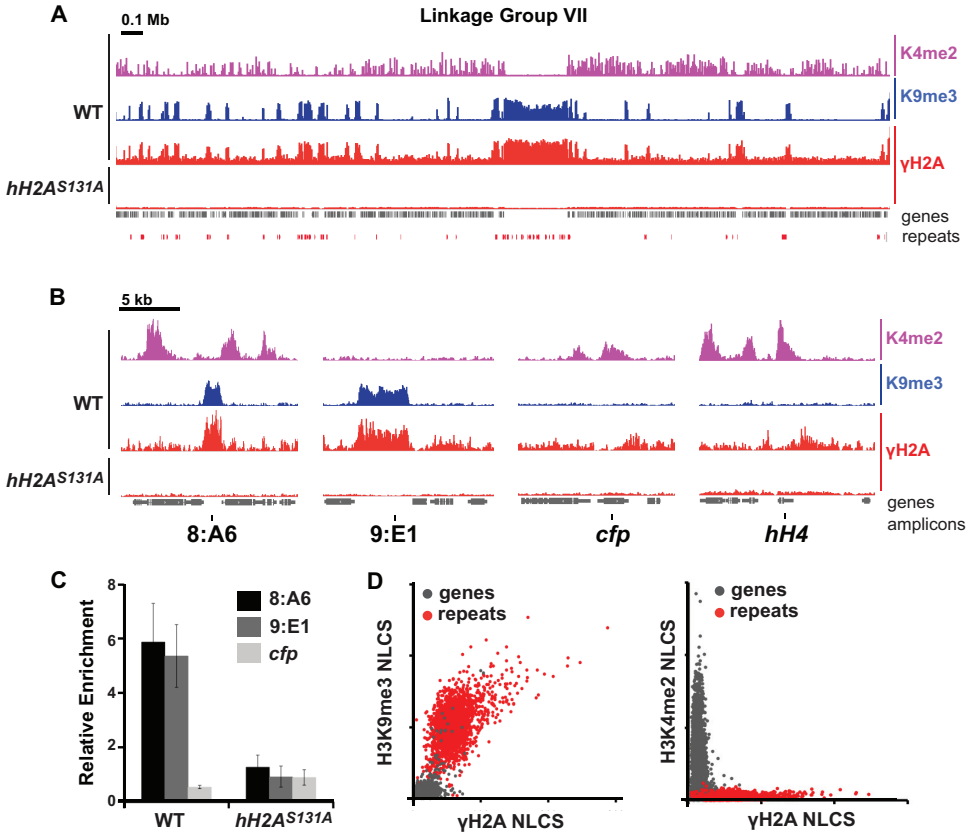

FIG 1 γH2A is a heterochromatin component in *Neurospora*. (A) ChIP-seq enrichment across linkage group VII is shown for H3K4me2, H3K9me3, and γH2A in the wild-type (WT) strain and for γH2A in the negative-control $hH2A^{S131A}$ strain. The strain is indicated to the left of the histogram, and the antibody used to perform ChIP-seq is indicated on the right. The positions of genes (gray) and degenerate DNA repeats (red) are shown at the bottom of the plot. (B) ChIP-seq enrichment patterns for representative heterochromatin (8:A6 and 9:E1) and euchromatin (*H4* and *cfp*) domains. Genes are shown in gray beneath each plot. The positions of PCR amplicons used to validate enrichment are indicated with a black line beneath each plot. (C) Quantitative real-time PCR analysis of the representative regions shown in panel B. The relative enrichment values for 8:A6, 9:E1, and *cfp* were determined by normalizing the indicated region to the *hH4* gene. Enrichment values for the wild-type and $hH2A^{S131A}$ strains were statistically different for the 8:A6 and 9:E1 regions (Student's *t* test; $P < 2.7 \times 10^{-6}$ and $P < 3.8 \times 10^{-8}$, respectively). (D) Scatterplots comparing enrichment of γH2A and H3K9me3 (left) or γH2A and H3K4me2 (right). The normalized ChIP enrichment value (NLCS) obtained for the indicated antibody was plotted for each genomic feature. Data for genes and tRNAs are shown in gray, and those for repeats are shown in red.

significantly reduced at all heterochromatin domains (see Fig. S2B in the supplemental material). Consistent with this apparent loss of enrichment, plotting the kernel density for γH2A enrichment in the *dim-5* strain revealed a single peak corresponding to uniform background enrichment across the genome for all features. We performed qPCR to validate the ChIP-seq data for representative heterochromatin domains on linkage groups (LG) II and V (Fig. 2E). We used primers to test enrichment adjacent to each domain (regions 90-1 and 230-1), at the edge of each domain (regions 90-2 and 230-2), and in the center of each domain (regions 90-3 and 230-3). qPCR data were fully consistent with the ChIP-seq data. γH2A enrichment was significantly reduced at both domains tested (peak 90 and peak 230) (see Table S3); however, a low level of γH2A in the center of the heterochromatin region remained (Fig. 2F) (Student's *t* test; $P < 0.008$ for region 90-2, $P < 0.008$ for region 90-3, $P < 0.0002$ for region 230-2, and $P < 0.007$ for region 230-3). Together, these data suggest that γH2A localization is altered in the *dim-5* mutant strain. We next asked if γH2A enrichment depends on H3K9me3. It was previously reported that H3K9 is an essential residue in *Neurospora*, based on the observation that H3K9L mutants were not recovered from crosses in which the mutant *hH3* allele was integrated at an ectopic locus (51). We constructed H3K9-to-arginine (R) and H3K9-to-glutamine (Q) replacement alleles, which mimic unacetylated and acetylated lysine, respectively. Homokaryons were obtained for both alleles, demonstrating that H3K9 is not essential (see Fig. S3 in the supplemental material). As expected, both H3K9 substitution strains lacked DNA methylation (see Fig. S3), indicating that heterochromatin formation was defective. Both strains also exhibited severe growth defects, similar to *dim-5* strains (see Fig. S4). We next performed ChIP-seq experiments with these H3K9me3-deficient strains. Like the case in *dim-5* strains, γH2A was no longer enriched in repetitive sequences in these mutants (Fig. 3A and B). Loss of enrichment was evident across the entire genome (see Fig. S2C). Data for three representative heterochromatin regions are shown in Fig. 3B. We confirmed these data by performing ChIP-qPCR to assay γH2A enrichment at the 8:A6 heterochromatin region (Fig. 3C) (Student's *t* test; $P < 4 \times 10^{-5}$ for the $hH3^{K9Q}$ mutant and $P < 1.5 \times 10^{-5}$ for the $hH3^{K9R}$ mutant). These data show that heterochromatin for-

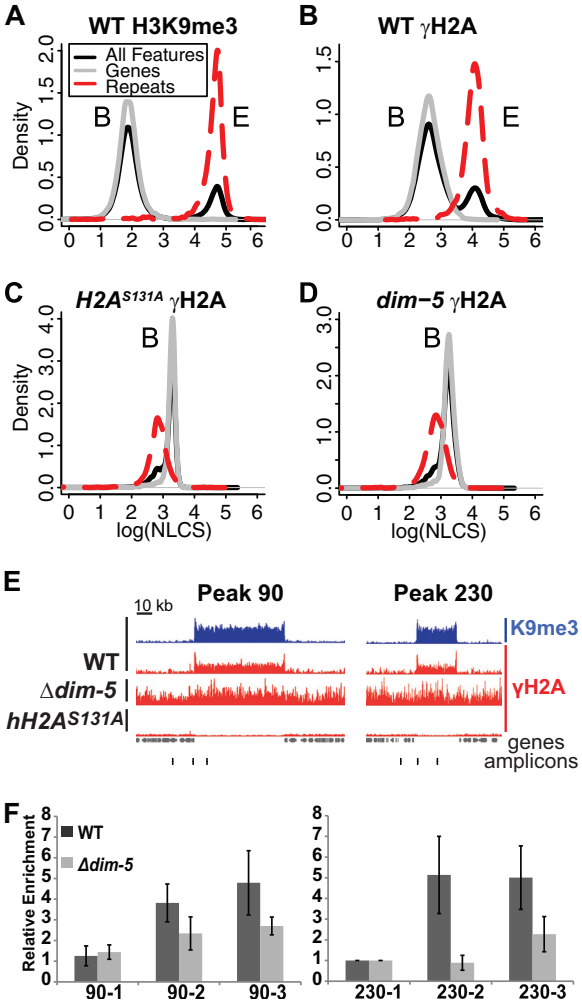

FIG 2 Enrichment of γH2A depends on DIM-5. (A to D) The distributions (kernel density estimations; densities) of normalized read counts (NLCS values) are shown for all genomic features (genes and repeats; black), genes only (gray), and repeats only (red). For the wild type, two peaks are observed for both H3K9me3 and γH2A, corresponding to features with background signals (peak B; genes) and features enriched in the modification (peak E; repeats). For the *hH2A*^{S131A} and Δ*dim-5* strains, all features exhibited background levels of γH2A enrichment. (E) ChIP-seq data for H3K9me3 and γH2A are shown for wild-type, Δ*dim-5*, and *hH2A*^{S131A} strains at two representative regions. The strain is indicated to the left of the histogram, and the antibody used to perform ChIP-seq is indicated on the right. Genes are shown in gray beneath each plot. The positions of PCR amplicons used to validate the ChIP-seq experiment are indicated with black lines beneath the plot. (F) γH2A ChIP samples were subjected to qPCR to analyze enrichment at each of the amplicons shown in panel E. Relative enrichment was determined by normalizing the enrichment value at each region to the euchromatic flank adjacent to each peak (region 90-1 or 230-1).

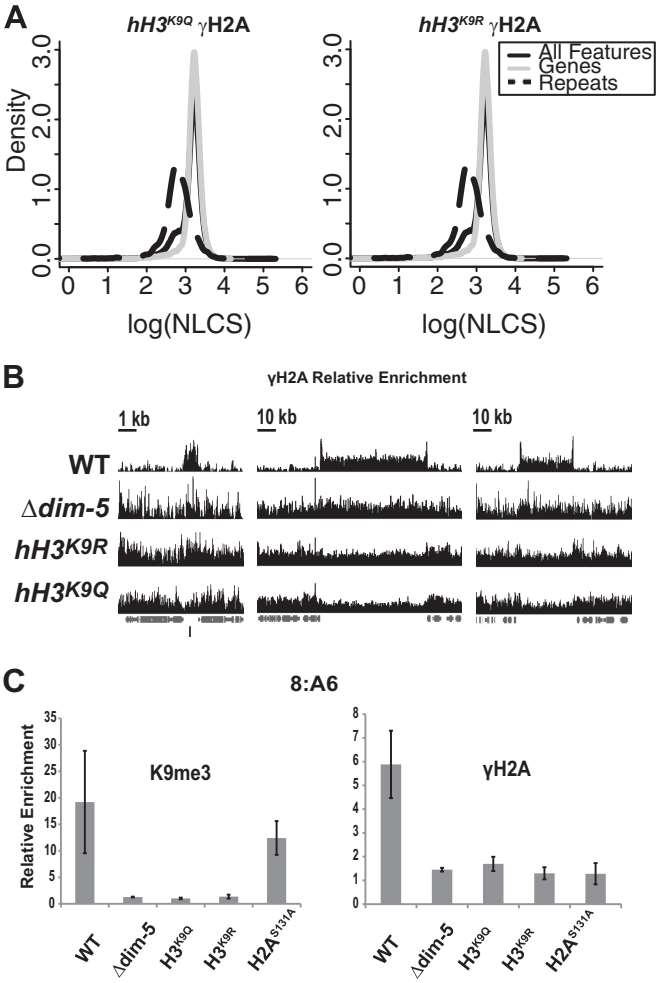

FIG 3 H3K9me3 is required for γH2A enrichment. (A) The distributions (kernel density estimations; densities) of normalized read counts (NLCS) are shown for all genomic features (genes and repeats), genes only, and repeats only for strains harboring H3K9 substitution alleles. In both strains, all features displayed equivalent background levels of γH2A enrichment. (B) ChIP-seq data for γH2A are shown for the wild-type and Δ*dim-5* strains and for two strains harboring H3K9 substitution alleles at two representative regions (peak 90 and peak 230). A scale bar at the top of each graph indicates the size of the region plotted. Genes are shown in gray beneath each plot. The position of the 8:A6 PCR amplicon used to validate the ChIP-seq experiment is indicated with a black line beneath the plot. (C) γH2A ChIP samples were subjected to qPCR to analyze enrichment at the 8:A6 region. Relative enrichment was determined by normalizing the enrichment value at 8:A6 to that at the *hH4* gene.

mation directed by DIM-5 is required for normal localization of γH2A.

Normal γH2A localization depends on HP1. HP1 binds methylated H3K9 and functions as a molecular scaffold to recruit additional chromatin-modifying enzymes to heterochromatin domains (21). *Neurospora* HP1 forms distinct complexes with the histone deacetylase HDA1 and the DNA methyltransferase (MTase) DIM-2 (22, 54). To determine if HP1, HDA1, or DIM-2 is required for proper control of γH2A localization, we performed ChIP-qPCR experiments using deletion strains that lack these proteins. As expected based on prior work, enrichment of H3K9me3 was abolished at the 8:A6 region in the *hpo* and *hda-1* strains but not in the *dim-2* strain. Similarly, γH2A was lost from the 8:A6 region in the *hpo* and *hda-1* strains but not in the *dim-2* strain (Fig. 4A) (Student's *t* test; $P < 0.0001$ for the *hpo* strain and $P < 1.0 \times 10^{-7}$ for the *hda-1* strain). We also performed qPCR to examine γH2A enrichment at the same representative regions on LGII and LGV as those examined above (peaks 90 and 230). For both regions, γH2A enrichment was lost at the edge of the heterochromatin domain in the *hpo* and *hda-1* strains (Student's *t* test; $P < 0.001$ for region 90-2 in the *hpo* strain, $P < 0.001$ for region 90-2 in the *hda-1* strain, $P < 0.002$ for region 230-2 in the *hda-1*

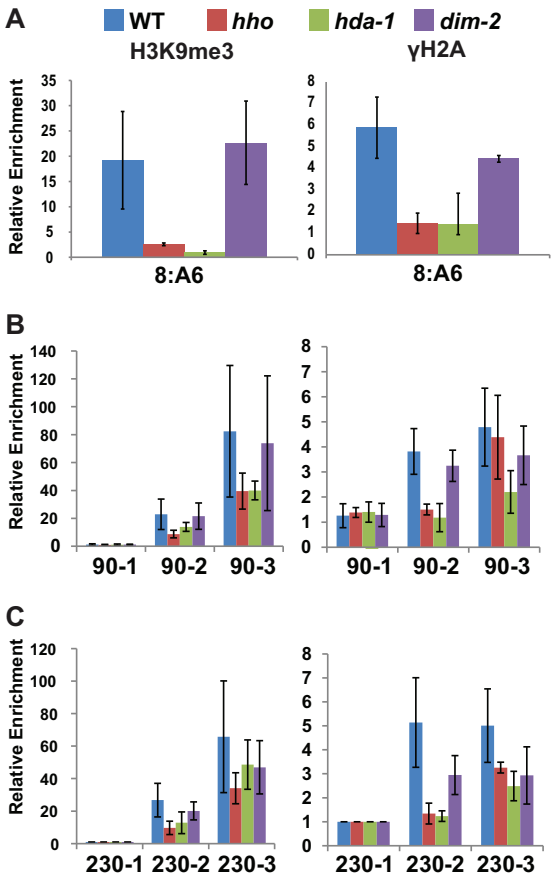

FIG 4 γH2A enrichment is reduced in the *hpo* and *hda-1* strains. ChIP was performed for the indicated strains, using antibodies to H3K9me3 (left) and γH2A (right). Relative enrichment levels at the 8:A6 region (A) and at sites within and adjacent to peak 90 (B) and peak 230 (C) were determined by qPCR. Enrichment at the 8:A6 region is shown relative to that at the euchromatic *hH4* gene. Enrichment values for peaks 90 and 230 are shown relative to the euchromatin region adjacent to each peak (PCR amplicons 90-1 and 230-1, respectively).

strain, and $P < 0.003$ for region 230-2 in the *hpo* strain). The *dim-2* strain exhibited a small decrease in γH2A enrichment at the edge of the LGV domain (region 230-2), but the observed difference was not statistically significant. The *dim-2* strain also failed to exhibit significant differences in the level of γH2A enrichment in the centers of these heterochromatin domains (Fig. 4B and C). Enrichment was slightly reduced in the centers of the LGII and LGV regions in the *hda-1* strain (Fig. 4C) (Student's *t* test; $P < 0.013$ for region 90-3 and $P < 0.025$ for region 230-3). Enrichment appeared to be slightly reduced in the middle of the LGV domain in the *hpo* strains, but this difference was not statistically significant (Fig. 4C) (Student's *t* test; $P < 0.17$ for region 230-3). These data suggest that the HCHC complex contributes to normal localization of γH2A. However, the loss of enrichment in the HCHC-deficient strains was less severe than that in the *dim-5* mutants at the regions tested. This suggests that another H3K9me-binding protein may be important for normal γH2A localization. In contrast, DNA methylation is not required for γH2A enrichment at heterochromatin domains.

γH2A is not required for H3K9 methylation or DNA methylation. Since γH2A is enriched in heterochromatin domains, we tested the possibility that γH2A regulates H3K9me3 or DNA methylation. qPCR experiments revealed similar enrichments of H3K9me3 at the 8:A6 region in both wild-type and $hH2A^{S131A}$ strains (Fig. 3C). To confirm this, we performed ChIP-seq experiments to examine H3K9me3 in the $hH2A^{S131A}$ strain. These analyses revealed that H3K9 methylation patterns were qualitatively similar in the wild type and the $hH2A^{S131A}$ strain (Fig. 5A). To next determine if γH2A was required for proper control of DNA methylation, genomic DNAs from the wild-type and $hH2A^{S131A}$ strains were digested with the methylation-sensitive enzyme BfuCI and the methylation-insensitive isoschizomer DpnII. The digested DNAs were analyzed by Southern blotting to examine DNA methylation at known methylated regions (8:A6, 8:G3, and centromere VII) (71). The membrane was also probed for the unmethylated

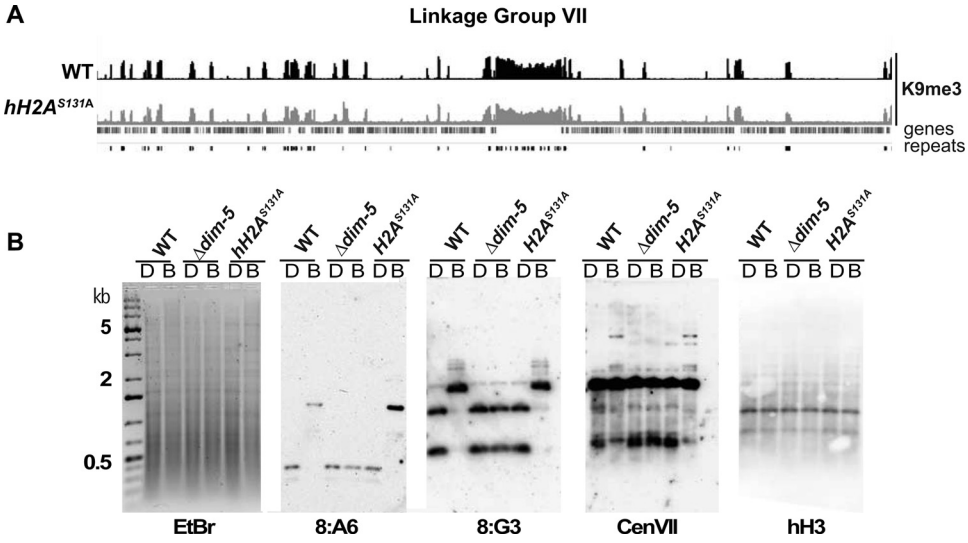

FIG 5 Heterochromatin formation is independent of γH2A. (A) ChIP-seq enrichment across linkage group VII is shown for H3K9me3 in the wild-type strain and the $hH2A^{S131A}$ strain. The strain is indicated to the left of the histogram. Genes are shown in gray, and degenerate DNA repeats are shown in black at the bottom of the plot. (B) Genomic DNAs from the wild-type, Δ*dim-5*, and $hH2A^{S131A}$ strains were digested with methylation-sensitive BfuCI (lanes B) and methylation-insensitive DpnII (lanes D). Cytosine methylation levels were analyzed by visualizing digested DNA with ethidium bromide (EtBr) and by probing Southern blots with the indicated methylated (8:A6, 8:G3, and centromere VII [CenVII]) and unmethylated (*hH3*) regions.

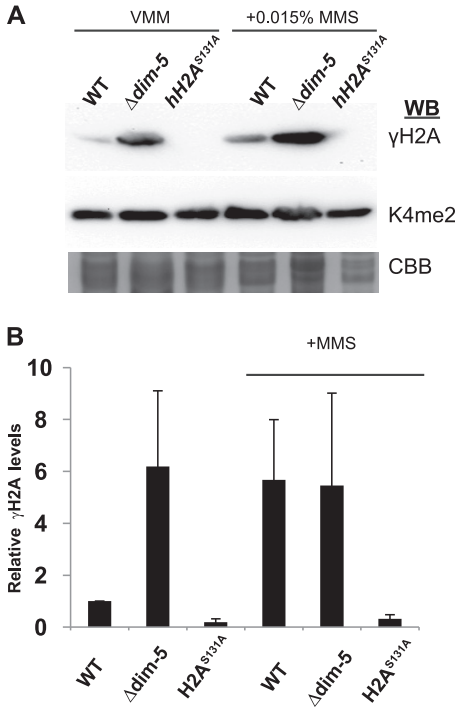

FIG 6 γH2A levels are elevated in the Δ*dim-5* strain. (A) Histones were isolated from the indicated strains grown in VMM or VMM plus 0.015% MMS and subjected to Western blot analyses (WB) of γH2A. As a loading control, Western blotting was performed using antibodies to H3K4me2, and gels were stained with Coomassie brilliant blue (CBB). (B) The levels of γH2A for each strain were determined by densitometry and normalized to those of H3K4me2 for each strain grown in VMM and VMM plus MMS.

H3 gene to confirm that the DNAs had been digested completely. Wild-type patterns of DNA methylation were observed for all four loci (Fig. 5B). These data show that γH2A is not required for H3K9 trimethylation or cytosine DNA methylation.

γH2A is induced in the *dim-5* strain. We asked if the loss of γH2A enrichment observed in the *dim-5* strain corresponded to a global reduction in γH2A levels. We isolated total histones from the wild-type, *dim-5*, and $hH2A^{S131A}$ strains. As a control, we also isolated histones from the same strains following exposure to the DNA-damaging agent MMS, and we performed Western blotting to examine the level of γH2A in each strain. To ensure equal loading, gels were stained with Coomassie brilliant blue, and we performed Western blotting using antibodies that recognize H3K4me2, which was previously demonstrated to be unchanged in the *dim-5* background (54). In the wild type, γH2A levels are low in minimal medium, but exposure to MMS leads to induction of γH2A, as observed previously (66). In contrast, analysis of the *dim-5* strain revealed that γH2A levels were significantly elevated in minimal medium (Student's *t* test; $P = 0.02$). γH2A levels remained high following exposure to MMS (Fig. 6). No signal was observed for the $hH2A^{S131A}$ strain.

These data appeared to be inconsistent with our ChIP-seq data, which suggested an apparent loss of enrichment in the *dim-5*, $H3^{K9R}$, and $H3^{K9Q}$ strains (Fig. 2 and 3). However, overall increased γH2A levels in euchromatin would also result in the loss of relative γH2A enrichment observed in H3K9me3-deficient strains. To test this possibility, we performed immunofluorescence assays to visualize γH2A localization in the wild-type and *dim-5* strains. Both strains contained an H1-RFP reporter construct to enable visualization of nuclei. In wild-type cells, the observed fluorescence was similar to that for the $hH2A^{S131A}$ strain, consistent with the low levels of γH2A observed in Western blot experiments (Fig. 7A; see Fig. S4 in the supplemental material). In contrast, nuclei in *dim-5* cells were intensely stained with the γH2A antibody (Fig. 7A). γH2A appeared to be enriched throughout *dim-5* nuclei, although some nuclei displayed nonuniform γH2A staining (Fig. 7B). Immunofluorescence assays revealed that γH2A accumulated in wild-type nuclei following exposure to the DNA-damaging agent MMS (see Fig. S5), demonstrating that this method is able to detect elevated levels of γH2A in wild-type cells. We quantified green and red fluorescence in wild-type and *dim-5* nuclei grown in minimal medium (Fig. 7C). These data confirmed that *dim-5* strains exhibit a significant induction of γH2A under normal growth conditions, consistent with defective DNA replication or repair in these strains. We next asked if γH2A misregulation is responsible for the drug sensitivity of *dim-5* strains. We tested colony survival of wild-type, *dim-5*, $hH2A^{S131A}$, and *dim-5*; $hH2A^{S131A}$ strains on MMS and the topoisomerase inhibitor camptothecin. Double-mutant strains were more sensitive than either single mutant, suggesting that DIM-5 regulates additional factors, along with γH2A, to promote proper DNA replication or repair (see Fig. S6).

DISCUSSION

γH2A associates with heterochromatin in *Neurospora*. We found that γH2A is a component of heterochromatin domains in wild-type *Neurospora* cells. Similar results were observed in *S. cerevisiae* and *S. pombe* (43, 45, 72), suggesting that γH2A is a conserved heterochromatin component in fungi, or at least in the ascomycetes. These data raise the possibility that γH2A is enriched in heterochromatin in other eukaryotes as well. Like the case in other organisms that have been studied, *Neurospora* γH2A is generated by ATM and ATR kinases in response to replication stress or DNA damage (66, 67). The MRN complex (Mre11, Rad50, and Nbs1) orchestrates ATM recruitment and activation at double-strand breaks (73, 74), while ATR is activated by accumulation of single-stranded DNA (ssDNA) (75). Because ssDNA can accumulate during various repair processes, ATR is able to respond to a variety of different types of DNA damage and genotoxic stresses. For example, ssDNA is generated during end resection of a double-strand break and at stalled replication forks, where the replicative helicase is thought to become uncoupled from DNA polymerase (76). It is possible that the heterochromatin structure leads to stalled replication forks in the wild type, thereby activating ATR kinase. Studies from *S. cerevisiae* show that γH2A overlaps regions that stall replication forks, including heterochromatin domains, and that recruitment of γH2A to heterochromatin depends on Sir3 (43, 72, 77). In *S. pombe*, heterochromatin-associated γH2A depends on the checkpoint kinase RAD3 (a homolog of ATR) (45). Certain DNA-binding proteins can inhibit replication fork progression (5). Thus, the tightly packaged nucleosomes found in heterochromatin may act as a natural impediment to replication forks. Indeed, analysis of replication intermediates by two-dimensional gel electrophoresis revealed stalled replication forks in heterochromatin domains of wild-type *S. pombe* cells (24). However, it remains possible that H2A kinases, such as ATR and ATM, are recruited directly to heterochromatin domains. Further studies

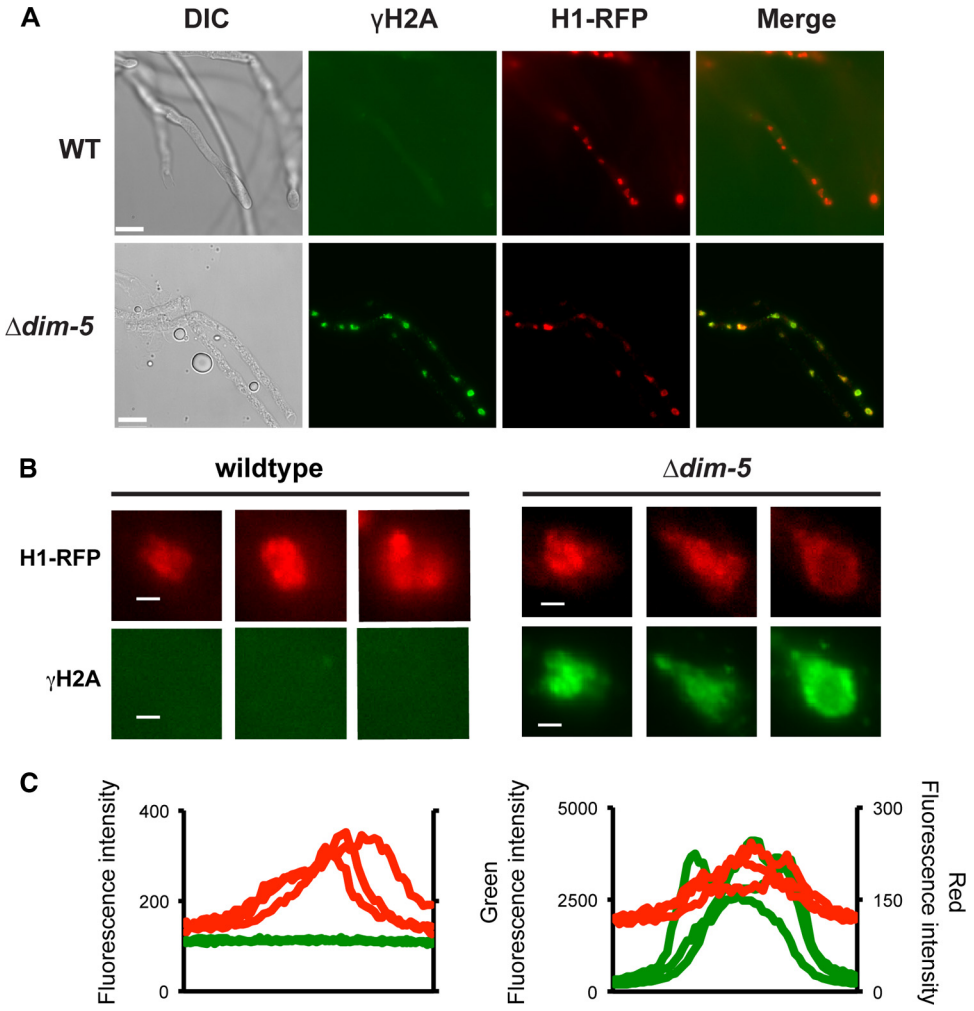

FIG 7 γH2A levels are elevated throughout Δ*dim-5* nuclei. (A) Immunofluorescence of γH2A is shown for wild-type and Δ*dim-5* cells. Both strains expressed an H1-dTomato fusion protein to allow visualization of nuclei (H1-RFP). Bars, 10 μm. (B) Immunofluorescence data for three individual nuclei from each strain. Bars, 1 μm. (C) Red and green fluorescence was quantified for three representative nuclei by using the SoftWorx Explorer "line profile" tool. The plots show fluorescence intensities measured along a 4-μm-line drawn across the center of the nucleus.

are needed to determine the mechanisms responsible for γH2A deposition in heterochromatin in wild-type cells.

In yeasts and animals, γH2A functions as a signal to recruit proteins that stabilize stalled replication forks or regulate DNA repair (41, 78, 79). For example, *S. pombe* Brc1 binds to γH2A via its BRCT domains to enable recovery from replication stress (78). *Neurospora* heterochromatin domains are comprised of AT-rich repetitive sequences that can adopt non-B-form DNA structures, such as cruciforms or hairpins. Such structures are known to stall replication forks in bacterial, yeast, and mammalian cells (80). It is therefore possible that γH2A functions to recruit proteins to stabilize replication forks that encounter natural sequence impediments found in heterochromatin domains. On the other hand, repeated DNA sequences can also provide substrates for illegitimate recombination, leading to chromosome rearrangements. Work with *Drosophila* revealed distinct DSB repair mechanisms in heterochromatin and euchromatin (32). The *Neurospora dim-5* mutant exhibits elevated rates of illegitimate recombination between heterochromatin-associated transgenes arranged in tandem (81). Thus, γH2A may recruit proteins to regulate the type of DNA repair that occurs in heterochromatin. The mammalian γH2A-binding protein PTIP binds 53BP1 to suppress homologous recombination (HR) and promote nonhomologous end joining (NHEJ) (82, 83), consistent with this possibility. The *Neurospora* genome encodes 10 BRCT domain-containing proteins (11). Future studies are required to determine if any of these proteins are localized to heterochromatin and, if so, what functions they might perform at these genomic regions.

While γH2A is best known for its response to replication stress and DNA damage, it is possible that this modified histone performs other functions at heterochromatin domains. Recent work with *S. cerevisiae* suggested that γH2A is important for long-range interactions between silent mating-type loci (77), raising the possibility that γH2A contributes to three-dimensional organization of the nucleus. On the other hand, γH2A may play a role in transcriptional silencing. The mammalian γH2A-binding protein MDC1 (mediator of DNA damage checkpoint 1) appears to be important for silencing sex chromosomes during male meiosis (84). In *S. cerevisiae*, the homolog of Brc1, Esc4/Rtt107, was implicated in silencing because it binds to the silencing protein SIR3

(85). In *S. pombe*, the γH2A-binding protein Brc1 is required for normal transcriptional silencing of a reporter gene embedded in pericentromeric heterochromatin (86). It is likely, however, that this protein contributes to silencing independently of γH2A, as γH2A itself is not required for silencing or for normal heterochromatin formation in *S. pombe* (45). We found that γH2A is not required for normal H3K9me3 or DNA methylation in *Neurospora*, demonstrating that heterochromatin formation does not depend on phosphorylation of H2A serine-131. In particular, we found that DNA methylation at the 8:A6 region is not affected in the *Neurospora* $H2A^{S131A}$ mutant. This result suggests that γH2A is not required for transcriptional silencing, because this locus frequently loses DNA methylation in mutants that affect transcriptional silencing (15, 22, 54).

Heterochromatin formation is required for normal genome stability in *Neurospora*. The DCDC complex is required for growth on the DNA-damaging agent MMS (16), suggesting that this complex is required for normal DNA replication or repair. In this study, we found that Δ*dim-5* strains have high levels of γH2A during normal replicative growth. These data suggest that Δ*dim-5* strains suffer spontaneous DNA damage during replication, perhaps due to frequent replication fork collapse. γH2A in *S. cerevisiae* and *S. pombe* heterochromatin-deficient mutants has been analyzed by ChIP. *S. cerevisiae sir3* mutants show reduced enrichment of γH2A in heterochromatin (72), and for *S. pombe*, it was reported that γH2A enrichment in centromeres and subtelomeric regions depends on Clr4, a homolog of $DIM\text{-}5^{KMT1}$ (45, 87). Based on the results obtained with *S. pombe*, it was suggested that H3K9 methylation by Clr4 is required for γH2A deposition in heterochromatin. Similarly, we observed reduced enrichment of γH2A at heterochromatin domains in the Δ*dim-5* strain. Taken together, our results suggest that heterochromatin-deficient *Neurospora* mutants do not exhibit reduced γH2A in heterochromatin but, rather, display elevated levels of γH2A throughout the genome. This interpretation is fully consistent with our global analyses of γH2A by Western blotting and immunofluorescence assays, as well as with our ChIP-seq analyses. It is possible that *S. pombe* heterochromatin mutants display a similar induction of γH2A. The reported loss of heterochromatin-associated γH2A in Clr4 mutants was determined by normalizing γH2A enrichment in heterochromatin domains to a euchromatic control locus. Thus, in *S. pombe*, loss of enrichment may result from increased γH2A in euchromatin, as observed in our experiments. This would be consistent with recent work showing that heterochromatin components are required for proper genome integrity of centromeres in the absence of fork stability components (88).

In *Drosophila* mutants lacking the DIM-5 homolog Su(var)3-9, γH2A is induced in foci that colocalize with heterochromatin (26, 27). Our results show that γH2A is dramatically induced in the *dim-5* strain and appears to be found throughout the nucleus. Given that γH2A is induced by stalled replication forks and by DSBs, these data suggest that DIM-5 is required for DNA replication or repair in *Neurospora*. This interpretation is supported by previous work demonstrating that DIM-5-deficient cells are hypersensitive to the DNA-damaging agent MMS (16). It is possible that DIM-5 is a global regulator of genome stability. However, γH2A is deposited in extremely large domains around DSBs (0.5 to 2 Mb in human cells) (42). In yeast, γH2A can spread to the undamaged domains close to the site of damage both in *cis* and in *trans*, presumably because ATR modifies serine-129 of H2A in close proximity (89). Our results may indicate that the Δ*dim-5* strain accumulates DSBs in heterochromatin domains, leading to massive spread of γH2A into euchromatin. Such a model is supported by recent analyses of *Drosophila* mutants defective for H3K9 methylation (4, 26, 27). These *Drosophila* mutants exhibit spontaneous DNA damage, including double-strand breaks, and suffer frequent genome rearrangements. These defects are presumably due to defective replication of heterochromatin-associated repeat sequences. Future studies are required to determine how heterochromatin might function to preserve genome integrity. The *Neurospora* genome includes abundant heterochromatin domains that share important molecular features with higher eukaryotes. Given these similarities with other eukaryotes, future work with *Neurospora* is likely to lead to important insights regarding the relationships between heterochromatin and genome maintenance.

ACKNOWLEDGMENTS

We thank Shin Hatakeyama and Shuuitsu Tanaka at Saitama University for providing the $H2A^{S131A}$ strain.

This work was funded in part by a grant to Z.A.L. from the March of Dimes Foundation (grant 5-FY14-89) and by a grant to M.F. from the National Institutes of Health (grant GM097637).

REFERENCES

1. **Grewal SI, Jia S.** 2007. Heterochromatin revisited. Nat. Rev. Genet. **8:**35–46. http://dx.doi.org/10.1038/nrg2008.
2. **McMurray CT.** 2010. Mechanisms of trinucleotide repeat instability during human development. Nat. Rev. Genet. **11:**786–799. http://dx.doi.org/10.1038/nrg2828.
3. **Lopez Castel A, Cleary JD, Pearson CE.** 2010. Repeat instability as the basis for human diseases and as a potential target for therapy. Nat. Rev. Mol. Cell Biol. **11:**165–170. http://dx.doi.org/10.1038/nrm2854.
4. **Peng J, Karpen G.** 2008. Epigenetic regulation of heterochromatic DNA stability. Curr. Opin. Genet. Dev. **18:**204–211. http://dx.doi.org/10.1016/j.gde.2008.01.021.
5. **Mirkin EV, Mirkin SM.** 2007. Replication fork stalling at natural impediments. Microbiol. Mol. Biol. Rev. **71:**13–35. http://dx.doi.org/10.1128/MMBR.00030-06.
6. **Mirkin SM.** 2006. DNA structures, repeat expansions and human hereditary disorders. Curr. Opin. Struct. Biol. **16:**351–358. http://dx.doi.org/10.1016/j.sbi.2006.05.004.
7. **Thompson SL, Compton DA.** 2011. Chromosomes and cancer cells. Chromosome Res. **19:**433–444. http://dx.doi.org/10.1007/s10577-010-9179-y.
8. **Dillon LW, Burrow AA, Wang YH.** 2010. DNA instability at chromosomal fragile sites in cancer. Curr. Genomics **11:**326–337. http://dx.doi.org/10.2174/138920210791616699.
9. **Hoskins RA, Carlson JW, Kennedy C, Acevedo D, Evans-Holm M, Frise E, Wan KH, Park S, Mendez-Lago M, Rossi F, Villasante A, Dimitri P, Karpen GH, Celniker SE.** 2007. Sequence finishing and mapping of *Drosophila melanogaster* heterochromatin. Science **316:**1625–1628. http://dx.doi.org/10.1126/science.1139816.
10. **Rabinowicz PD, Bennetzen JL.** 2006. The maize genome as a model for efficient sequence analysis of large plant genomes. Curr. Opin. Plant Biol. **9:**149–156. http://dx.doi.org/10.1016/j.pbi.2006.01.015.
11. **Galagan JE, et al.** 2003. The genome sequence of the filamentous fungus *Neurospora crassa*. Nature **422:**859–868. http://dx.doi.org/10.1038/nature01554.
12. **Lander ES, et al.** 2001. Initial sequencing and analysis of the human genome. Nature **409:**860–921. http://dx.doi.org/10.1038/35057062.
13. **Cleveland DW, Mao Y, Sullivan KF.** 2003. Centromeres and kinetochores: from epigenetics to mitotic checkpoint signaling. Cell **112:**407–421. http://dx.doi.org/10.1016/S0092-8674(03)00115-6.
14. **Smith KM, Phatale PA, Sullivan CM, Pomraning KR, Freitag M.** 2011. Heterochromatin is required for normal distribution of *Neurospora crassa* CenH3. Mol. Cell. Biol. **31:**2528–2542. http://dx.doi.org/10.1128/MCB.01285-10.

15. **Lewis ZA, Honda S, Khlafallah TK, Jeffress JK, Freitag M, Mohn F, Schubeler D, Selker EU.** 2009. Relics of repeat-induced point mutation direct heterochromatin formation in *Neurospora crassa*. Genome Res. **19:** 427–437. http://dx.doi.org/10.1101/gr.086231.108.
16. **Lewis ZA, Adhvaryu KK, Honda S, Shiver AL, Knip M, Sack R, Selker EU.** 2010. DNA methylation and normal chromosome behavior in Neurospora depend on five components of a histone methyltransferase complex, DCDC. PLoS Genet. **6:**e1001196. http://dx.doi.org/10.1371/journal.pgen.1001196.
17. **Lewis ZA, Adhvaryu KK, Honda S, Shiver AL, Selker EU.** 2010. Identification of DIM-7, a protein required to target the DIM-5 H3 methyltransferase to chromatin. Proc. Natl. Acad. Sci. U. S. A. **107:**8310–8315. http://dx.doi.org/10.1073/pnas.1000328107.
18. **Xu H, Wang J, Hu Q, Quan Y, Chen H, Cao Y, Li C, Wang Y, He Q.** 2010. DCAF26, an adaptor protein of Cul4-based E3, is essential for DNA methylation in *Neurospora crassa*. PLoS Genet. **6:**e1001132. http://dx.doi.org/10.1371/journal.pgen.1001132.
19. **Zhao Y, Shen Y, Yang S, Wang J, Hu Q, Wang Y, He Q.** 2010. Ubiquitin ligase components Cullin4 and DDB1 are essential for DNA methylation in *Neurospora crassa*. J. Biol. Chem. **285:**4355–4365. http://dx.doi.org/10.1074/jbc.M109.034710.
20. **Allis CD, Berger SL, Cote J, Dent Jenuwien ST, Kouzarides T, Pillus L, Reinberg D, Shi Y, Shiekhattar R, Shilatifard A, Workman J, Zhang Y.** 2007. New nomenclature for chromatin-modifying enzymes. Cell **131:** 633–636. http://dx.doi.org/10.1016/j.cell.2007.10.039.
21. **Freitag M, Hickey PC, Khlafallah TK, Read ND, Selker EU.** 2004. HP1 is essential for DNA methylation in Neurospora. Mol. Cell **13:**427–434. http://dx.doi.org/10.1016/S1097-2765(04)00024-3.
22. **Honda S, Lewis ZA, Shimada K, Fischle W, Sack R, Selker EU.** 2012. Heterochromatin protein 1 forms distinct complexes to direct histone deacetylation and DNA methylation. Nat. Struct. Mol. Biol. **19:**471–477. http://dx.doi.org/10.1038/nsmb.2274.
23. **Honda S, Lewis ZA, Huarte M, Cho LY, David LL, Shi Y, Selker EU.** 2010. The DMM complex prevents spreading of DNA methylation from transposons to nearby genes in *Neurospora crassa*. Genes Dev. **24:**443–454. http://dx.doi.org/10.1101/gad.1893210.
24. **Zaratiegui M, Castel SE, Irvine DV, Kloc A, Ren J, Li F, de Castro E, Marin L, Chang AY, Goto D, Cande WZ, Antequera F, Arcangioli B, Martienssen RA.** 2011. RNAi promotes heterochromatic silencing through replication-coupled release of RNA Pol II. Nature **479:**135–138. http://dx.doi.org/10.1038/nature10501.
25. **Cam HP, Sugiyama T, Chen ES, Chen X, FitzGerald PC, Grewal SI.** 2005. Comprehensive analysis of heterochromatin- and RNAi-mediated epigenetic control of the fission yeast genome. Nat. Genet. **37:**809–819. http://dx.doi.org/10.1038/ng1602.
26. **Peng JC, Karpen GH.** 2009. Heterochromatic genome stability requires regulators of histone H3 K9 methylation. PLoS Genet. **5:**e1000435. http://dx.doi.org/10.1371/journal.pgen.1000435.
27. **Peng JC, Karpen GH.** 2007. H3K9 methylation and RNA interference regulate nucleolar organization and repeated DNA stability. Nat. Cell Biol. **9:**25–35. http://dx.doi.org/10.1038/ncb1514.
28. **Paredes S, Maggert KA.** 2009. Ribosomal DNA contributes to global chromatin regulation. Proc. Natl. Acad. Sci. U. S. A. **106:**17829–17834. http://dx.doi.org/10.1073/pnas.0906811106.
29. **Soria G, Almouzni G.** 2013. Differential contribution of HP1 proteins to DNA end resection and homology-directed repair. Cell Cycle **12:**422–429. http://dx.doi.org/10.4161/cc.23215.
30. **Lee YH, Kuo CY, Stark JM, Shih HM, Ann DK.** 2013. HP1 promotes tumor suppressor BRCA1 functions during the DNA damage response. Nucleic Acids Res. **41:**5784–5798. http://dx.doi.org/10.1093/nar/gkt231.
31. **Bolderson E, Savage KI, Mahen R, Pisupati V, Graham ME, Richard DJ, Robinson PJ, Venkitaraman AR, Khanna KK.** 2012. Kruppel-associated box (KRAB)-associated co-repressor (KAP-1) Ser-473 phosphorylation regulates heterochromatin protein 1beta (HP1-beta) mobilization and DNA repair in heterochromatin. J. Biol. Chem. **287:**28122–28131. http://dx.doi.org/10.1074/jbc.M112.368381.
32. **Chiolo I, Minoda A, Colmenares SU, Polyzos A, Costes SV, Karpen GH.** 2011. Double-strand breaks in heterochromatin move outside of a dynamic HP1a domain to complete recombinational repair. Cell **144:**732–744. http://dx.doi.org/10.1016/j.cell.2011.02.012.
33. **Baldeyron C, Soria G, Roche D, Cook AJ, Almouzni G.** 2011. HP1alpha recruitment to DNA damage by p150CAF-1 promotes homologous recombination repair. J. Cell Biol. **193:**81–95. http://dx.doi.org/10.1083/jcb.201101030.
34. **Luijsterburg MS, Dinant C, Lans H, Stap J, Wiernasz E, Lagerwerf S, Warmerdam DO, Lindh M, Brink MC, Dobrucki JW, Aten JA, Fousteri MI, Jansen G, Dantuma NP, Vermeulen W, Mullenders LH, Houtsmuller AB, Verschure PJ, van Driel R.** 2009. Heterochromatin protein 1 is recruited to various types of DNA damage. J. Cell Biol. **185:**577–586. http://dx.doi.org/10.1083/jcb.200810035.
35. **Dinant C, Luijsterburg MS.** 2009. The emerging role of HP1 in the DNA damage response. Mol. Cell. Biol. **29:**6335–6340. http://dx.doi.org/10.1128/MCB.01048-09.
36. **Quivy JP, Gerard A, Cook AJ, Roche D, Almouzni G.** 2008. The HP1-p150/CAF-1 interaction is required for pericentric heterochromatin replication and S-phase progression in mouse cells. Nat. Struct. Mol. Biol. **15:**972–979. http://dx.doi.org/10.1038/nsmb.1470.
37. **Ayoub N, Jeyasekharan AD, Bernal JA, Venkitaraman AR.** 2008. HP1-beta mobilization promotes chromatin changes that initiate the DNA damage response. Nature **453:**682–686. http://dx.doi.org/10.1038/nature06875.
38. **Liu H, Galka M, Mori E, Liu X, Lin YF, Wei R, Pittock P, Voss C, Dhami G, Li X, Miyaji M, Lajoie G, Chen B, Li SS.** 2013. A method for systematic mapping of protein lysine methylation identifies functions for HP1beta in DNA damage response. Mol. Cell **50:**723–735. http://dx.doi.org/10.1016/j.molcel.2013.04.025.
39. **Dickey JS, Redon CE, Nakamura AJ, Baird BJ, Sedelnikova OA, Bonner WM.** 2009. H2AX: functional roles and potential applications. Chromosoma **118:**683–692. http://dx.doi.org/10.1007/s00412-009-0234-4.
40. **Downs JA, Lowndes NF, Jackson SP.** 2000. A role for *Saccharomyces cerevisiae* histone H2A in DNA repair. Nature **408:**1001–1004. http://dx.doi.org/10.1038/35050000.
41. **Paull TT, Rogakou EP, Yamazaki V, Kirchgessner CU, Gellert M, Bonner WM.** 2000. A critical role for histone H2AX in recruitment of repair factors to nuclear foci after DNA damage. Curr. Biol. **10:**886–895. http://dx.doi.org/10.1016/S0960-9822(00)00610-2.
42. **Iacovoni JS, Caron P, Lassadi I, Nicolas E, Massip L, Trouche D, Legube G.** 2010. High-resolution profiling of gammaH2AX around DNA double strand breaks in the mammalian genome. EMBO J. **29:**1446–1457. http://dx.doi.org/10.1038/emboj.2010.38.
43. **Szilard RK, Jacques PE, Laramee L, Cheng B, Galicia S, Bataille AR, Yeung M, Mendez M, Bergeron M, Robert F, Durocher D.** 2010. Systematic identification of fragile sites via genome-wide location analysis of gamma-H2AX. Nat. Struct. Mol. Biol. **17:**299–305. http://dx.doi.org/10.1038/nsmb.1754.
44. **Rogakou EP, Pilch DR, Orr AH, Ivanova VS, Bonner WM.** 1998. DNA double-stranded breaks induce histone H2AX phosphorylation on serine 139. J. Biol. Chem. **273:**5858–5868. http://dx.doi.org/10.1074/jbc.273.10.5858.
45. **Rozenzhak S, Mejia-Ramirez E, Williams JS, Schaffer L, Hammond JA, Head SR, Russell P.** 2010. Rad3 decorates critical chromosomal domains with gammaH2A to protect genome integrity during S-phase in fission yeast. PLoS Genet. **6:**e1001032. http://dx.doi.org/10.1371/journal.pgen.1001032.
46. **Davis RH.** 2000. Neurospora: contributions of a model organism. Oxford University Press, Oxford, United Kingdom.
47. **Pall ML.** 1993. The use of Ignite (Basta; glufosinate; phosphinothricin) to select transformants of bar-containing plasmids in Neurospora crassa. Fungal Genet. Newsl. **40:**58.
48. **Sambrook J, Russell DW.** 2001. Molecular cloning: a laboratory manual, 3rd ed. Cold Spring Harbor Laboratory Press, Cold Spring Harbor, NY.
49. **Liu H, Naismith JH.** 2008. An efficient one-step site-directed deletion, insertion, single and multiple-site plasmid mutagenesis protocol. BMC Biotechnol. **8:**91. http://dx.doi.org/10.1186/1472-6750-8-91.
50. **Tamaru H, Selker EU.** 2001. A histone H3 methyltransferase controls DNA methylation in *Neurospora crassa*. Nature **414:**277–283. http://dx.doi.org/10.1038/35104508.
51. **Adhvaryu KK, Berge E, Tamaru H, Freitag M, Selker EU.** 2011. Substitutions in the amino-terminal tail of Neurospora histone H3 have varied effects on DNA methylation. PLoS Genet. **7:**e1002423. http://dx.doi.org/10.1371/journal.pgen.1002423.
52. **Margolin BS, Freitag M, Selker EU.** 1997. Improved plasmids for gene targeting at the his-3 locus of *Neurospora crassa* by electroporation. Fungal Genet. Newsl. **44:**34–36.
53. **Pomraning KR, Smith KM, Freitag M.** 2009. Genome-wide high

throughput analysis of DNA methylation in eukaryotes. Methods **47:**142–150. http://dx.doi.org/10.1016/j.ymeth.2008.09.022.
54. **Honda S, Selker EU.** 2008. Direct interaction between DNA methyltransferase DIM-2 and HP1 is required for DNA methylation in *Neurospora crassa*. Mol. Cell. Biol. **28:**6044–6055. http://dx.doi.org/10.1128/MCB.00823-08.
55. **Miao VP, Freitag M, Selker EU.** 2000. Short TpA-rich segments of the zeta-eta region induce DNA methylation in *Neurospora crassa*. J. Mol. Biol. **300:**249–273. http://dx.doi.org/10.1006/jmbi.2000.3864.
56. **Langmead B, Salzberg SL.** 2012. Fast gapped-read alignment with Bowtie 2. Nat. Methods **9:**357–359. http://dx.doi.org/10.1038/nmeth.1923.
57. **Thorvaldsdottir H, Robinson JT, Mesirov JP.** 2013. Integrative Genomics Viewer (IGV): high-performance genomics data visualization and exploration. Brief. Bioinform. **14:**178–192. http://dx.doi.org/10.1093/bib/bbs017.
58. **Robinson JT, Thorvaldsdottir H, Winckler W, Guttman M, Lander ES, Getz G, Mesirov JP.** 2011. Integrative genomics viewer. Nat. Biotechnol. **29:**24–26. http://dx.doi.org/10.1038/nbt.1754.
59. **Price AL, Jones NC, Pevzner PA.** 2005. De novo identification of repeat families in large genomes. Bioinformatics **21**(Suppl 1):i351–i358. http://dx.doi.org/10.1093/bioinformatics/bti1018.
60. **Kent WJ.** 2002. BLAT—the BLAST-like alignment tool. Genome Res. **12:**656–664. http://dx.doi.org/10.1101/gr.229202.
61. **Hebenstreit D, Gu M, Haider S, Turner DJ, Lio P, Teichmann SA.** 2011. EpiChIP: gene-by-gene quantification of epigenetic modification levels. Nucleic Acids Res. **39:**e27. http://dx.doi.org/10.1093/nar/gkq1226.
62. **Quinlan AR, Hall IM.** 2010. BEDTools: a flexible suite of utilities for comparing genomic features. Bioinformatics **26:**841–842. http://dx.doi.org/10.1093/bioinformatics/btq033.
63. **Momany M.** 2001. Using microscopy to explore the duplication cycle, p 119–125. *In* Talbot N (ed), Molecular and cell biology of filamentous fungi: a practical approach. Oxford University Press, Oxford, United Kingdom.
64. **Scott JH, Schekman R.** 1980. Lyticase: endoglucanase and protease activities that act together in yeast cell lysis. J. Bacteriol. **142:**414–423.
65. **Ward IM, Chen J.** 2001. Histone H2AX is phosphorylated in an ATR-dependent manner in response to replicational stress. J. Biol. Chem. **276:**47759–47762. http://dx.doi.org/10.1074/jbc.C100569200.
66. **Wakabayashi M, Saijyou N, Hatakeyama S, Inoue H, Tanaka S.** 2012. Neurospora mrc1 homologue is involved in replication stability and is required for normal cell growth and chromosome integrity in mus-9 and mus-21 mutants. Fungal Genet. Biol. **49:**263–270. http://dx.doi.org/10.1016/j.fgb.2012.02.007.
67. **Wakabayashi M, Ishii C, Hatakeyama S, Inoue H, Tanaka S.** 2010. ATM and ATR homologues of Neurospora crassa are essential for normal cell growth and maintenance of chromosome integrity. Fungal Genet. Biol. **47:**809–817. http://dx.doi.org/10.1016/j.fgb.2010.05.010.
68. **Oyola SO, Otto TD, Gu Y, Maslen G, Manske M, Campino S, Turner DJ, Macinnis B, Kwiatkowski DP, Swerdlow HP, Quail MA.** 2012. Optimizing Illumina next-generation sequencing library preparation for extremely AT-biased genomes. BMC Genomics **13:**1. http://dx.doi.org/10.1186/1471-2164-13-1.
69. **Aird D, Ross MG, Chen WS, Danielsson M, Fennell T, Russ C, Jaffe DB, Nusbaum C, Gnirke A.** 2011. Analyzing and minimizing PCR amplification bias in Illumina sequencing libraries. Genome Biol. **12:**R18. http://dx.doi.org/10.1186/gb-2011-12-2-r18.
70. **Tamaru H, Zhang X, McMillen D, Singh PB, Nakayama J, Grewal SI, Allis CD, Cheng X, Selker EU.** 2003. Trimethylated lysine 9 of histone H3 is a mark for DNA methylation in *Neurospora crassa*. Nat. Genet. **34:**75–79. http://dx.doi.org/10.1038/ng1143.
71. **Selker EU, Tountas NA, Cross SH, Margolin BS, Murphy JG, Bird AP, Freitag M.** 2003. The methylated component of the *Neurospora crassa* genome. Nature **422:**893–897. http://dx.doi.org/10.1038/nature01564.
72. **Kitada T, Schleker T, Sperling AS, Xie W, Gasser SM, Grunstein M.** 2011. gammaH2A is a component of yeast heterochromatin required for telomere elongation. Cell Cycle **10:**293–300. http://dx.doi.org/10.4161/cc.10.2.14536.
73. **Lee JH, Paull TT.** 2005. ATM activation by DNA double-strand breaks through the Mre11-Rad50-Nbs1 complex. Science **308:**551–554. http://dx.doi.org/10.1126/science.1108297.
74. **Lee JH, Paull TT.** 2004. Direct activation of the ATM protein kinase by the Mre11/Rad50/Nbs1 complex. Science **304:**93–96. http://dx.doi.org/10.1126/science.1091496.
75. **Byun TS, Pacek M, Yee MC, Walter JC, Cimprich KA.** 2005. Functional uncoupling of MCM helicase and DNA polymerase activities activates the ATR-dependent checkpoint. Genes Dev. **19:**1040–1052. http://dx.doi.org/10.1101/gad.1301205.
76. **Zeman MK, Cimprich KA.** 2014. Causes and consequences of replication stress. Nat. Cell Biol. **16:**2–9. http://dx.doi.org/10.1038/ncb2897.
77. **Kirkland JG, Kamakaka RT.** 2013. Long-range heterochromatin association is mediated by silencing and double-strand DNA break repair proteins. J. Cell Biol. **201:**809–826. http://dx.doi.org/10.1083/jcb.201211105.
78. **Williams JS, Williams RS, Dovey CL, Guenther G, Tainer JA, Russell P.** 2010. gammaH2A binds Brc1 to maintain genome integrity during S-phase. EMBO J. **29:**1136–1148. http://dx.doi.org/10.1038/emboj.2009.413.
79. **Li X, Liu K, Li F, Wang J, Huang H, Wu J, Shi Y.** 2012. Structure of C-terminal tandem BRCT repeats of Rtt107 protein reveals critical role in interaction with phosphorylated histone H2A during DNA damage repair. J. Biol. Chem. **287:**9137–9146. http://dx.doi.org/10.1074/jbc.M111.311860.
80. **Voineagu I, Narayanan V, Lobachev KS, Mirkin SM.** 2008. Replication stalling at unstable inverted repeats: interplay between DNA hairpins and fork stabilizing proteins. Proc. Natl. Acad. Sci. U. S. A. **105:**9936–9941. http://dx.doi.org/10.1073/pnas.0804510105.
81. **Chicas A, Forrest EC, Sepich S, Cogoni C, Macino G.** 2005. Small interfering RNAs that trigger posttranscriptional gene silencing are not required for the histone H3 Lys9 methylation necessary for transgenic tandem repeat stabilization in *Neurospora crassa*. Mol. Cell. Biol. **25:**3793–3801. http://dx.doi.org/10.1128/MCB.25.9.3793-3801.2005.
82. **Callen E, Di Virgilio M, Kruhlak MJ, Nieto-Soler M, Wong N, Chen HT, Faryabi RB, Polato F, Santos M, Starnes LM, Wesemann DR, Lee JE, Tubbs A, Sleckman BP, Daniel JA, Ge K, Alt FW, Fernandez-Capetillo O, Nussenzweig MC, Nussenzweig A.** 2013. 53BP1 mediates productive and mutagenic DNA repair through distinct phosphoprotein interactions. Cell **153:**1266–1280. http://dx.doi.org/10.1016/j.cell.2013.05.023.
83. **Yan W, Shao Z, Li F, Niu L, Shi Y, Teng M, Li X.** 2011. Structural basis of gammaH2AX recognition by human PTIP BRCT5-BRCT6 domains in the DNA damage response pathway. FEBS Lett. **585:**3874–3879. http://dx.doi.org/10.1016/j.febslet.2011.10.045.
84. **Ichijima Y, Ichijima M, Lou Z, Nussenzweig A, Camerini-Otero RD, Chen J, Andreassen PR, Namekawa SH.** 2011. MDC1 directs chromosome-wide silencing of the sex chromosomes in male germ cells. Genes Dev. **25:**959–971. http://dx.doi.org/10.1101/gad.2030811.
85. **Zappulla DC, Maharaj AS, Connelly JJ, Jockusch RA, Sternglanz R.** 2006. Rtt107/Esc4 binds silent chromatin and DNA repair proteins using different BRCT motifs. BMC Mol. Biol. **7:**40. http://dx.doi.org/10.1186/1471-2199-7-40.
86. **Lee SY, Rozenzhak S, Russell P.** 2013. gammaH2A-binding protein Brc1 affects centromere function in fission yeast. Mol. Cell. Biol. **33:**1410–1416. http://dx.doi.org/10.1128/MCB.01654-12.
87. **Lee SY, Russell P.** 2013. Brc1 links replication stress response and centromere function. Cell Cycle **12:**1665–1671. http://dx.doi.org/10.4161/cc.24900.
88. **Li PC, Petreaca RC, Jensen A, Yuan JP, Green MD, Forsburg SL.** 2013. Replication fork stability is essential for the maintenance of centromere integrity in the absence of heterochromatin. Cell Rep. **3:**638–645. http://dx.doi.org/10.1016/j.celrep.2013.02.007.
89. **Lee CS, Lee K, Legube G, Haber JE.** 2014. Dynamics of yeast histone H2A and H2B phosphorylation in response to a double-strand break. Nat. Struct. Mol. Biol. **21:**103–109. http://dx.doi.org/10.1038/nsmb.2737.